



Cite this: *New J. Chem.*, 2018, 42, 18189

Enhanced peroxidase-like activity of porphyrin functionalized ZnFe₂O₄ hollow nanospheres for rapid detection of H₂O₂ and glucose†

Bing Bian,^{ab} Qingyun Liu^{id}*^b and Shitao Yu*^a

Using a simple one-pot solvothermal method, binary metal oxide, magnetic and hollow ZnFe₂O₄ nanospheres functionalized with 5,10,15,20-tetrakis(4-carboxylphenyl)-porphyrin (Por-ZnFe₂O₄ HSs) were prepared and subsequently applied as a substitute for natural peroxidase. The Por-ZnFe₂O₄ HSs were characterized using powder X-ray diffraction (XRD), scanning electron microscopy (SEM), transmission electron microscopy (TEM) and X-ray photoelectron spectroscopy (XPS). In comparison with bare ZnFe₂O₄ HSs, Por-ZnFe₂O₄ HSs exhibit enhanced intrinsic peroxidase-like activity. They demonstrate a fast colorimetric response to H₂O₂ with a detection limit as low as 0.86 μM. The catalytic mechanism of the system was proved to be a hydroxyl radical mechanism using electron spin resonance (ESR). By combining the Por-ZnFe₂O₄ HSs-catalyzed reaction and the enzymatic oxidation of glucose with glucose oxidase, a colorimetric platform for glucose detection was established. The Por-ZnFe₂O₄ HSs/glucose oxidase (GOx)/TMB system shows a good response toward glucose with a detection limit of 5.5 μM. Therefore, such nanocomposites have promising applications in biomimetic catalysis and environmental monitoring.

Received 12th February 2018,
Accepted 4th October 2018

DOI: 10.1039/c8nj00720a

rsc.li/njc

1. Introduction

Due to their ease of preparation, tunable catalytic activity and high stability under harsh conditions, artificial enzymes, which function as good substitutes for natural enzymes, have been extensively applied in catalysis and bioassays in the past decade.¹ Nanomaterials have many unique properties such as large surface-to-volume ratio, high catalytic efficiency and high surface reaction activity. The pioneering work of Gao *et al.*,² who discovered the intrinsic peroxidase activity possessed by magnetic Fe₃O₄ nanoparticles, has paved a new way for exploiting novel enzyme mimetics. Since then, various nanoscale materials, such as metals,^{3–6} metal oxides,^{7–9} metal sulfides,^{10–13} carbon nanomaterials^{14–18} and organic compounds^{19–22} have been reported to possess intrinsic enzymatic activity. Many single-component catalysts usually demonstrate low catalytic efficiency, hampering their application in catalysis and biological fields. Subsequently, multi-component nanocomposites emerged with enhanced catalytic activity from the synergistic effect of their different components. Recently, hybrid nanocomposites such as

carbon-based nanosheets,^{23–25} core-shell nanoparticles,^{26–28} alloys^{29,30} and organic-inorganic nanocomposites^{31,32} have been developed as peroxidase mimetics. Despite the great progress, developing novel nanocomposites with improved peroxidase-like activity for biological applications is still challenging.

Among the various binary metal oxides, magnetic zinc ferrite magnetite (ZnFe₂O₄) has attracted enormous interest because of its outstanding properties including high stability, good dispersibility, ease of separation, high catalytic efficiency, and low toxicity of zinc ions.^{33–35} Additionally, ZnFe₂O₄ nanoparticles have intrinsic peroxidase-like catalytic activity and have been successfully used for the colorimetric detection of glucose in urine.³⁶ Unfortunately, the poor separation efficiency of electrons and holes in bare ZnFe₂O₄ nanoparticles causes low catalytic activity. To solve this problem, one efficient solution is to further functionalize the ZnFe₂O₄ nanoparticles and harness the synergistic effect between the different components to achieve high catalytic activity.

Porphyrins, which have two-dimensional 18 π-electron aromatic macrocycle structures, can be synthetically modified by introducing various functional groups or metal ions, leading to unique optical and electronic properties.^{37–39} Therefore, porphyrins can be adopted to functionalize nanostructures applied in solar energy conversion and photocatalysis.^{40,41} Numerous studies involving porphyrin⁴² and porphyrin functionalized nanomaterials⁴³ have been reported in the fields of

^a College of Chemical Engineering, Qingdao University of Science and Technology, Qingdao 266042, China. E-mail: yushitaoqust@126.com; Fax: +86 532 84022719; Tel: +86 532 84022719

^b College of Chemical and Environmental Engineering, Shandong University of Science and Technology, Qingdao 266510, China. E-mail: qyliu@sdu.edu.cn; Fax: +86 0532 80681197; Tel: +86 0532 86057757

† Electronic supplementary information (ESI) available. See DOI: 10.1039/c8nj00720a

biocatalysis and biosensors. Ju's group have synthesized free-base-porphyrin-functionalized ZnO nanoparticles on indium tin oxide for the detection of cysteine.⁴⁴ Our group previously reported that porphyrin functionalized monometal oxides, NiO, Fe₃O₄ and CeO₂,⁴⁵ and metal sulfides ZnS and CdS⁴⁶ demonstrated enhanced peroxidase-like activity to detect H₂O₂ and glucose. Nevertheless, to the best of our knowledge, the use of porphyrin functionalized binary metal oxide, ZnFe₂O₄, as a peroxidase mimic has not been reported yet.

In this work, 5,10,15,20-tetrakis(4-carboxylphenyl)-porphyrin functionalized hollow ZnFe₂O₄ nanospheres (Por-ZnFe₂O₄ HSS) were fabricated through a convenient one-pot hydrothermal process. The molecular structure of 5,10,15,20-tetrakis(4-carboxylphenyl)-porphyrin is shown in Fig. S1 (ESI[†]). The morphology and structure of the nanocomposites were systematically investigated. Owing to the synergistic effect of porphyrin and ZnFe₂O₄, the Por-ZnFe₂O₄ HSS exhibited enhanced peroxidase-like activity and rapidly catalyzed the colorless substrate 3,3',5,5'-tetramethylbenzidine (TMB) into a blue product (oxTMB), observed by the naked eye in only 3 min (Scheme 1). The catalytic mechanism of Por-ZnFe₂O₄ HSS was also investigated using electron spin resonance. Meanwhile, a rapid, sensitive and selective colorimetric method based on Por-ZnFe₂O₄ HSS for H₂O₂ and glucose determination was established.

2. Experimental

2.1. Reagents and apparatus

FeCl₃·6H₂O and ZnCl₂ were purchased from Beichen Fangzheng Reagent Co. (Tianjin, China). 3,3',5,5'-Tetramethylbenzidine dihydrochloride (TMB·2HCl) was ordered from Solarbio Co. (Beijing, China). Hydrogen peroxide H₂O₂ (30 wt%), sodium acetate (NaAc), glucose, fructose, lactose, maltose and sucrose were obtained from Guangcheng Reagent Co. (Tianjin, China). Ethylene glycol and PEG 20 000 were obtained from BASF Chemical Co., Ltd (Tianjin, China). 5,5-Dimethyl-1-pyrroline-*N*-oxide (DMPO) was purchased from J&K Chemical Ltd (Shanghai, China). Glucose oxidase (GOx, ≥200 U mg⁻¹) was purchased from Sigma-Aldrich and stored in a refrigerator at -18 °C. All reagents were of analytical grade and deionized water was used in all experiments. 5,10,15,20-Tetrakis(4-carboxylphenyl)-porphyrin (Por) was synthesized according to a previously reported method.⁴⁷

The samples were subjected to various physical characterization methods. Powder X-ray diffraction characterization

was carried out using a Rigaku D/Max2500PC powder X-ray diffractometer with Cu Kα radiation, a 2θ range of 5–80° and a scan rate of 5° min⁻¹. A JEM-2100 transmission electron microscope (JEOL, Japan) and a Nova Nano SEM450 scanning electron microscope (FEI, USA) were used to examine the morphology of the Por-ZnFe₂O₄ HSS. UV-vis absorption spectra were recorded on a UV-3200PC spectrophotometer (Shanghai, China). Fourier transform infrared (FT-IR) spectra were recorded on a NICOLET 380 FT-IR spectrometer (Nicolet Thermo, USA) in the range of 4000–500 cm⁻¹ using a KBr disk method. X-ray photoelectron spectroscopy (XPS) analysis was used to confirm the elemental composition using a PHI Quantum 2000 Scanning ESCA Microprobe spectrometer with an Al Kα incident X-ray beam. The X-ray source was operated at 35 W, and the spectra were recorded at 15 kV. The analysis chamber pressure was 5 × 10⁻⁸ Pa. The electron spin resonance (ESR) measurements were carried out with a Bruker ESP-300E spectrometer operating in the X-band at room temperature.

2.2. Preparation of magnetic Por-ZnFe₂O₄ HSS

In a typical process, hollow magnetic ZnFe₂O₄ nanospheres functionalized with porphyrin were synthesized through a one-step hydrothermal method. Briefly, ZnCl₂ (0.34 g, 2.5 mmol) and FeCl₃·6H₂O (1.35 g, 5 mmol) were dissolved in ethylene glycol (40 mL) to form a clear solution, followed by the addition of NaAc (3.6 g) and polyethylene glycol 20 000 (1.0 g). The color of the solution turned from bright yellow to clear dark brown. After addition of 5 mg 5,10,15,20-tetrakis(4-carboxylphenyl)-porphyrin, the mixture was stirred vigorously for 30 min. The mixture was then transferred into a 50 mL teflon-lined autoclave and incubated at 200 °C for 8 h. After cooling down, the obtained black precipitate was separated from the solvent using a magnet, washed several times with deionized water and ethanol, and then dried at 60 °C in a vacuum drying oven for 12 h.

Bare ZnFe₂O₄ hollow nanospheres were synthesized according to the above route without adding porphyrin.

2.3. Peroxidase-like catalytic activity and kinetics analysis study

Peroxidase-like catalytic activity and kinetics analysis were evaluated using the catalytic oxidation of 3,3',5,5'-tetramethylbenzidine (TMB) in the presence of H₂O₂ at room temperature. After adding 200 μL Por-ZnFe₂O₄ HSS stock solution, 200 μL 3 mM TMB and 200 μL 0.1 M H₂O₂ to 1400 μL 0.2 M acetate



Scheme 1 Schematic illustration of the colorimetric detection of glucose by combining GOx and Por-ZnFe₂O₄ nanospheres for catalyzed reactions.

buffer solution at pH 4.0 to form a total 2 mL mixture, reactions were monitored in time-scan mode at 652 nm. Kinetics measurements were carried out in time course mode by monitoring the absorbance change for 3 min on a UV-3200PC UV-vis spectrophotometer. The Michaelis–Menten constant was calculated using Lineweaver–Burk plots: $1/\nu = K_m/V_{\max}(1/[S] + 1/K_m)$, where ν is the initial velocity, V_{\max} is the maximum reaction velocity and $[S]$ is the concentration of the substrate. K_m is the Michaelis–Menten constant, which is an indicator of enzyme affinity for its substrate.

2.4. Electron spin resonance (ESR)

The catalytic mechanism of the Por-ZnFe₂O₄ HSs was investigated in the H₂O₂/UV/DMPO system in the presence and absence of Por-ZnFe₂O₄ HSs. Samples containing 18 mM DMPO, 25 mM H₂O₂, and different concentrations of the Por-ZnFe₂O₄ HSs (0, 60, 100 μg mL⁻¹) were prepared in acetate buffer (20 mM, pH 4.0). Each sample was UV irradiated at 365 nm for 10 min, transferred to a quartz capillary tube and placed in the ESR cavity for spectrum recording.

2.5. H₂O₂ and glucose detection using Por-ZnFe₂O₄ HSs

The colorimetric detection of H₂O₂ was performed as follows: 200 μL TMB (3 mM), 200 μL Por-ZnFe₂O₄ HSs stock solution (0.4 mg mL⁻¹) and 200 μL H₂O₂ with different concentrations were added into 1400 μL acetate buffer (pH 4.0) and incubated for 3 min at room temperature. The Por-ZnFe₂O₄ HSs were removed from the reaction mixture using an external magnetic field. UV-vis spectra were recorded by wavelength scanning. To examine the influences of pH and experimental temperature on the catalytic activity of Por-ZnFe₂O₄ HSs, buffer solutions from pH 2.0 to 9.0 and temperatures from 20 to 60 °C were investigated.

Glucose detection was carried out in the following steps: (1) 100 μL of 0.5 mg mL⁻¹ GOx and 500 μL of glucose with different concentrations in 0.01 M phosphate buffered saline (PBS, pH 7.0) were incubated at 37 °C for 30 min; (2) 200 μL of 3 mM TMB, 200 μL of the Por-ZnFe₂O₄ HSs (40 μg mL⁻¹) stock solution, and 1 mL of acetate buffer (pH 4.0) were added into the above incubated reaction; (3) the mixture was incubated in a 37 °C water bath for 10 min, and kept in an ice-water bath for another 10 min to terminate the reaction; (4) the Por-ZnFe₂O₄ HSs were then removed from the reaction solution using an external magnetic field and the final reaction solution was used to perform the absorption spectroscopy measurements at 652 nm. In control experiments, 5 mM maltose, 5 mM lactose, 5 mM sucrose and 5 mM fructose were used instead of glucose.

3. Results and discussion

3.1. Characterization of the Por-ZnFe₂O₄ HSs

XRD was employed to analyze the crystallographic nature of bare ZnFe₂O₄ HSs and Por-ZnFe₂O₄ HSs. Fig. 1 shows the characteristic diffraction peaks at 29.9°, 35.2°, 42.8°, 53.1°, 56.6° and 62.2°, corresponding to the (111), (220), (400), (422),

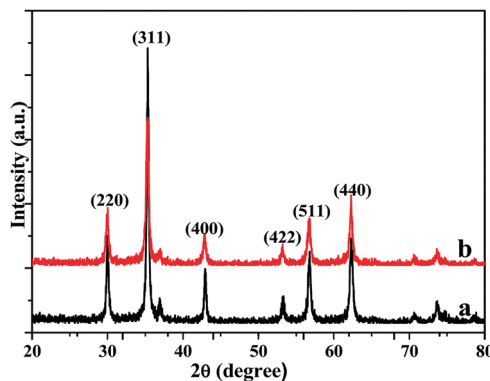


Fig. 1 XRD patterns of Por-ZnFe₂O₄ HSs (a) and bare ZnFe₂O₄ HSs (b).

(511) and (440) planes, respectively. Therefore, the characterized material can be assigned as ZnFe₂O₄ (JCPDS 22-1012) with a spinel structure. With the introduction of porphyrin molecules, the XRD pattern shows negligible change, suggesting that the formation of the nanocomposites does not influence the crystal structure of raw ZnFe₂O₄.

In order to determine the composition of the nanocomposites, XPS was used to further explore the chemical composition and surface electronic state of the Por-ZnFe₂O₄ HSs. The narrow-scanned XPS spectrum indicates the coexistence of Zn, Fe, O, C and N elements in the nanocomposites. The peak at 1021.2 eV was ascribed to Zn 2p_{3/2} (Fig. 2a). Fe 2p signals located at 711.1 eV and 725.2 eV should be attributed to the characteristic features of Fe 2p_{3/2} and Fe 2p_{1/2}, respectively (Fig. 2b). Furthermore, the O 1s spectrum displayed in Fig. 2c shows a peak at 530.0 eV that could be assigned to typical surface lattice oxygen. The C 1s (Fig. 2d) spectrum of Por-ZnFe₂O₄ HSs could be divided into three peaks, the main peak at 284.80 eV was due to adventitious carbon, which was used to calibrate binding energies, together with carbon from the porphyrin molecules. The peaks at 285.8 eV and 288.2 eV were attributed to the C=N and O=C=O bonds of the porphyrin molecules, respectively. Fig. 2e shows the spectrum of the N 1s regions with a peak at a binding energy of 399.7 eV. From the XPS spectra of C and N from the porphyrin molecules, it can be seen that porphyrin molecules exist in the Por-ZnFe₂O₄ HSs.

The functionalization of the ZnFe₂O₄ HSs by porphyrin was verified using the FT-IR spectra, shown in Fig. S2 (ESI†). The FT-IR of porphyrin (curve a) showed a signal at 1682 cm⁻¹, corresponding to the vibration of the carboxylic groups, and at 1423 cm⁻¹, corresponding to the vibration peak of an aromatic acid. Notably, from curve b, it can be found that the vibration of the carboxylic groups from the porphyrin molecule shifted to 1590 cm⁻¹ with a broad band, indicating that a coordination interaction occurred between the carbonyl groups of porphyrin and ZnFe₂O₄.

The morphology of the samples was analyzed using SEM and TEM. Fig. 3 shows typical SEM and TEM images of bare ZnFe₂O₄ HSs and Por-ZnFe₂O₄ HSs. Clearly, the obtained samples are both composed of hollow nanospheres with uniform shape and diameters from ca. 100 to 200 nm. Furthermore, it can be seen that the hollow nanospheres were composed of nanoparticles, as shown in Fig. 3(a and c). The hollow structure can be clearly

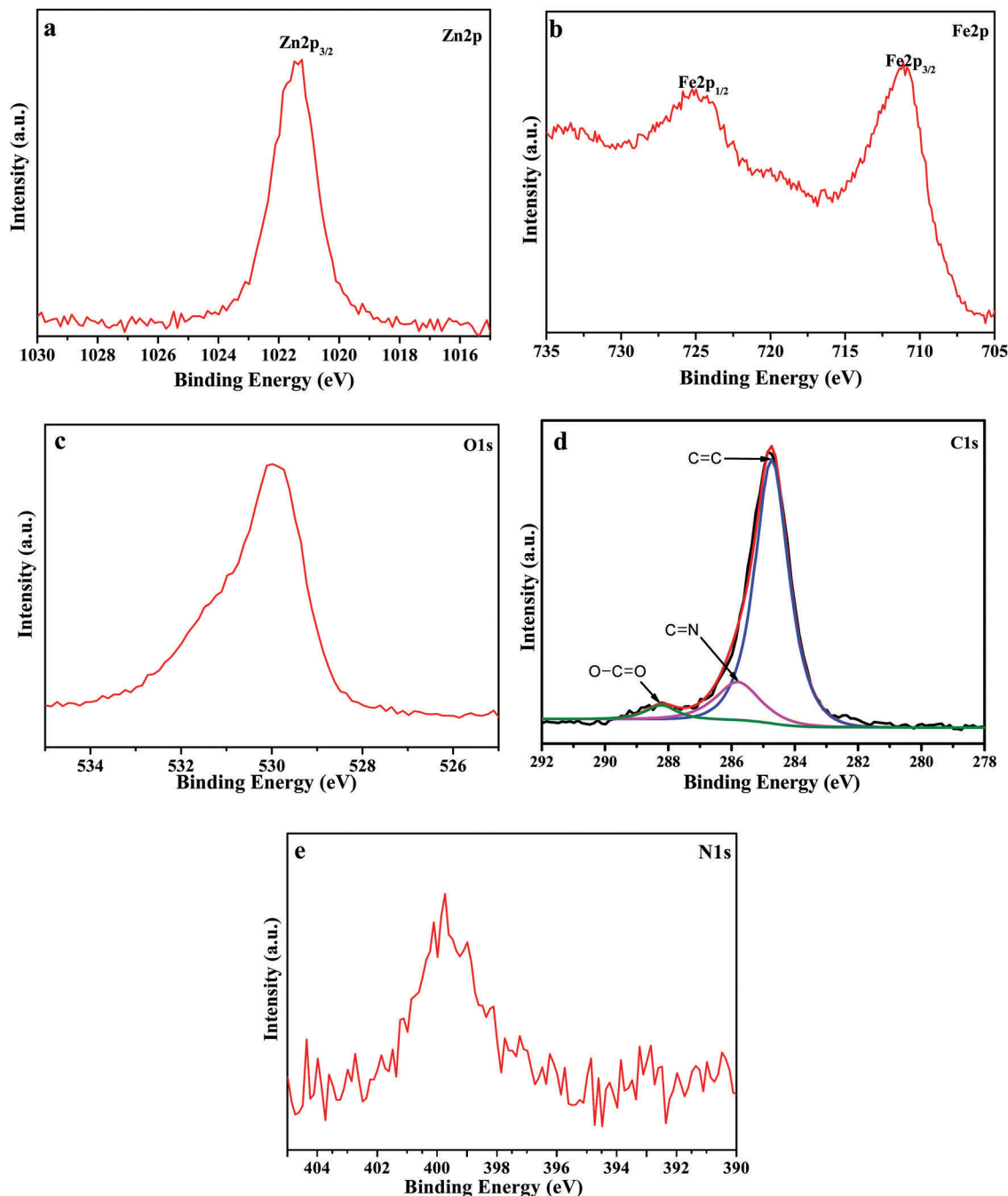


Fig. 2 XPS survey spectra of the Por-ZnFe₂O₄ HSs nanocomposites.

seen from a broken sphere, indicated by the arrow in Fig. 3c. From the SEM and TEM images of both bare ZnFe₂O₄ HSs and Por-ZnFe₂O₄ HSs, it can be suggested that the morphology of the ZnFe₂O₄ HSs was not affected by the 5,10,15,20-tetrakis(4-carboxylphenyl)-porphyrin, owing to a small quantity of porphyrin molecules attached on the surface of the hollow nanoparticles.

3.2. The peroxidase-like catalytic activity of magnetic Por-ZnFe₂O₄ HSs

In the presence of H₂O₂, natural peroxidases can catalyze the oxidation of 3,3',5,5'-tetramethylbenzidine (TMB) to produce a

significant blue color. To investigate the peroxidase-like catalytic activity of the Por-ZnFe₂O₄ HSs, catalytic oxidation of the chromogenic substrate TMB with Por-ZnFe₂O₄ HS nanocomposites in the presence or absence of H₂O₂ were investigated. With the addition of Por-ZnFe₂O₄ HSs into the TMB-H₂O₂ solution, an obvious change to a blue color occurs (Fig. 4e), suggesting the formation of Ox TMB catalyzed by Por-ZnFe₂O₄ HSs. In contrast, in the absence of H₂O₂, no obvious color change was observed in the TMB/Por-ZnFe₂O₄ HSs solution. All the results suggest that neither H₂O₂ nor the Por-ZnFe₂O₄ HSs alone could effectively oxidize TMB. It is the obtained

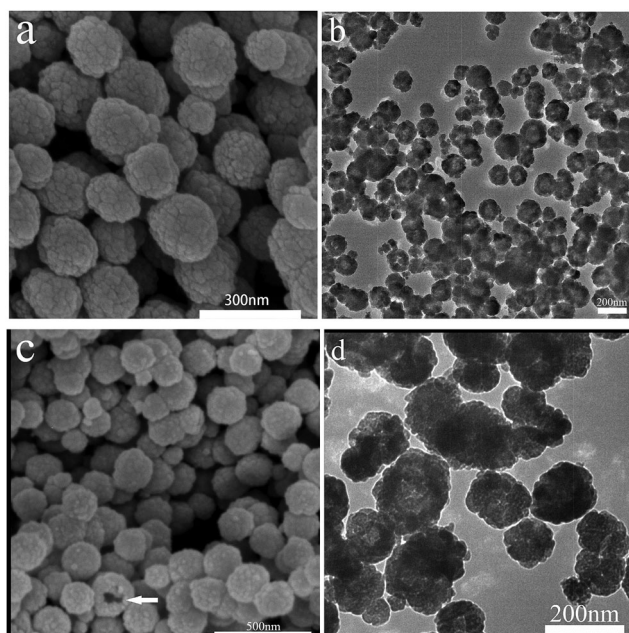


Fig. 3 (a) SEM and (b) TEM images of ZnFe_2O_4 HSs; (c) SEM (the arrow marks a broken hollow sphere) and (d) TEM images of Por- ZnFe_2O_4 HSs.

Por- ZnFe_2O_4 nanocomposites that have excellent peroxidase-like activity.

To compare the catalytic performance with that of bare ZnFe_2O_4 HSs, control experiments were performed. As shown in Fig. 4e, the solution in the presence of Por- ZnFe_2O_4 HSs, TMB and H_2O_2 shows an intense absorption at 652 nm and a deep color change. In contrast, under identical experimental conditions, the TMB + H_2O_2 + ZnFe_2O_4 HSs system shows slight color variation (Fig. 4d). The catalytic activity of Por- ZnFe_2O_4 HSs was about four times higher than that of bare ZnFe_2O_4 HSs. The time taken for different colorimetric reactions catalyzed by nanomaterials has been summarized and listed in Table 1. Clearly, compared with other nanomaterials such as Fe_3O_4

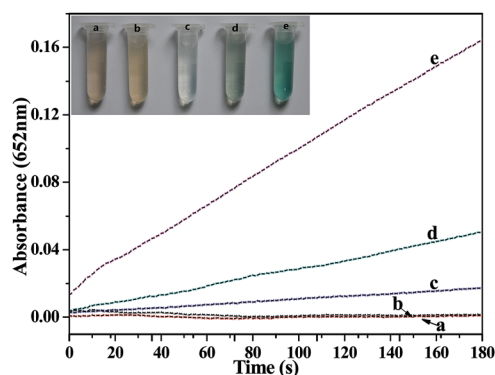


Fig. 4 Time-dependent absorbance changes at 652 nm of TMB in different reaction systems: (a) TMB + ZnFe_2O_4 HSs, (b) TMB + Por- ZnFe_2O_4 HSs, (c) TMB + H_2O_2 , (d) TMB + ZnFe_2O_4 HSs + H_2O_2 , and (e) TMB + Por- ZnFe_2O_4 HSs + H_2O_2 in a pH 4.0 acetate buffer at 35 °C. Inset are photographs of the color changes of the different samples.

Table 1 Time comparison of the color response time of substrates observed by the naked eye when adding Por- ZnFe_2O_4 HSs and other peroxidase mimetics

Catalyst	Reaction time (min)	Ref.
Fe_3O_4 MNPs	10	8
ZnFe_2O_4 MNPs	5	36
C-dots/NiAl-LDHs	10	48
GO- Fe_3O_4	15	49
$\text{H}_2\text{TCCP-CeO}_2$	15	45
$\text{H}_2\text{TCCP-ZnS}$	10	46
Por- ZnFe_2O_4 HSs	3	This work

MNPs, ZnFe_2O_4 MNPs, C-dots/NiAl-LDHs, and GO- Fe_3O_4 , Por- ZnFe_2O_4 HSs exhibit the highest catalytic activity.

3.3. Mechanism of the peroxidase-like activity of magnetic Por- ZnFe_2O_4 HSs

Generally, the catalytic mechanisms of peroxidase mimics could be classified into two types. One is from electron transfer, as seen in Ir and Co_3O_4 .^{5,7} The other is from hydroxyl radicals, which is seen in catalysts including Fe_3O_4 , CoFe_2O_4 and

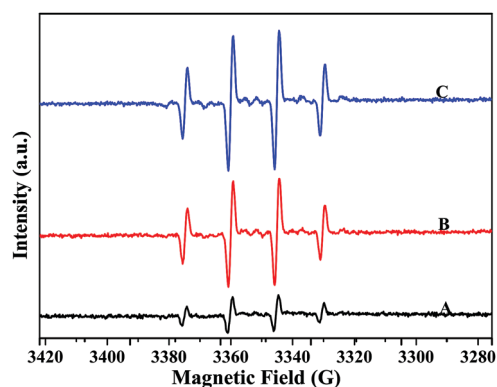
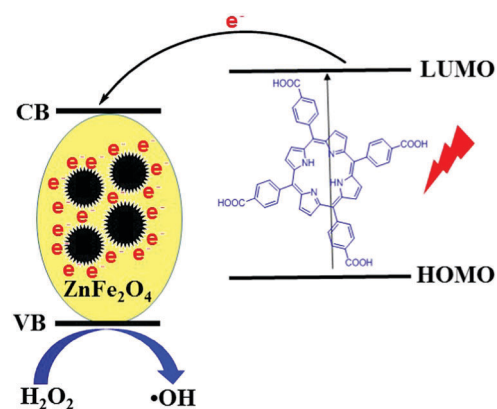


Fig. 5 Spin-trapping ESR spectra of $\cdot\text{OH}$ radicals in the systems of (A) H_2O_2 -DMPO, (B) $60 \mu\text{g mL}^{-1}$ Por- ZnFe_2O_4 HSs- H_2O_2 -DMPO and (C) $100 \mu\text{g mL}^{-1}$ Por- ZnFe_2O_4 HSs- H_2O_2 -DMPO. Reaction conditions: 18 mM DMPO, 25 mM H_2O_2 .



Scheme 2 Schematic energy level diagram and electron-transfer path from the porphyrin to ZnFe_2O_4 .

$\text{Fe}_3(\text{PO}_4)_2 \cdot 8\text{H}_2\text{O}$.⁵⁰ Based on previous reports, it is speculated that the excellent intrinsic peroxidase-like activity of Por-ZnFe₂O₄ HSSs could be ascribed to the generation of hydroxyl radicals ($\cdot\text{OH}$) from H₂O₂ in the process of the rapid oxidation of TMB. As a powerful method to characterize the hydroxyl radicals, the ESR technique was adopted to verify the generation of $\cdot\text{OH}$ with 5,5-dimethyl-1-pyrroline-*N*-oxide (DMPO) as a

spin trap. Fig. 5A shows four weak characteristic peaks of the typical DMPO- $\cdot\text{OH}$ adduct with an intensity ratio of 1:2:2:1. In contrast, strong ESR signals of the spin adduct are observed in Fig. 5B and C. It can be seen that the ESR signal of the spin adduct in the presence of 100 $\mu\text{g mL}^{-1}$ Por-ZnFe₂O₄ HSSs was stronger than that of 60 $\mu\text{g mL}^{-1}$ Por-ZnFe₂O₄ HSSs, suggesting that the spin adduct ESR intensity was dependent on the

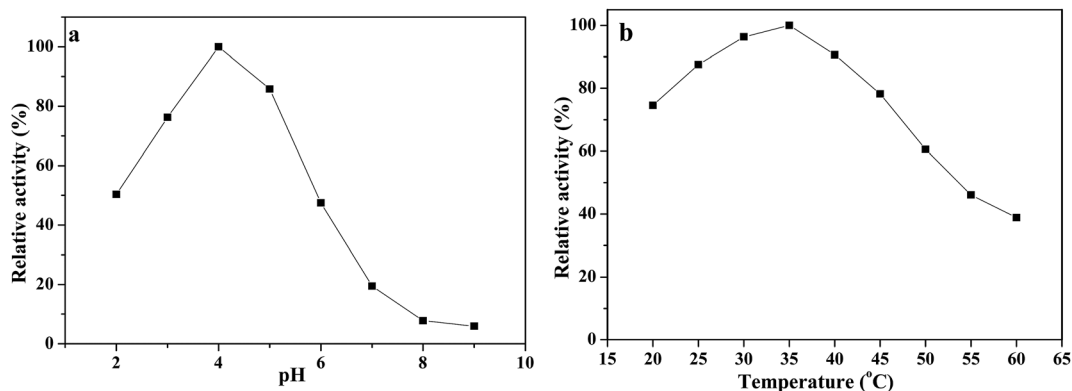


Fig. 6 The dependence of the peroxidase-like activity of the Por-ZnFe₂O₄ HSSs on (a) pH and (b) temperature in the presence of TMB and H₂O₂. The maximum point in each curve is set as 100%.

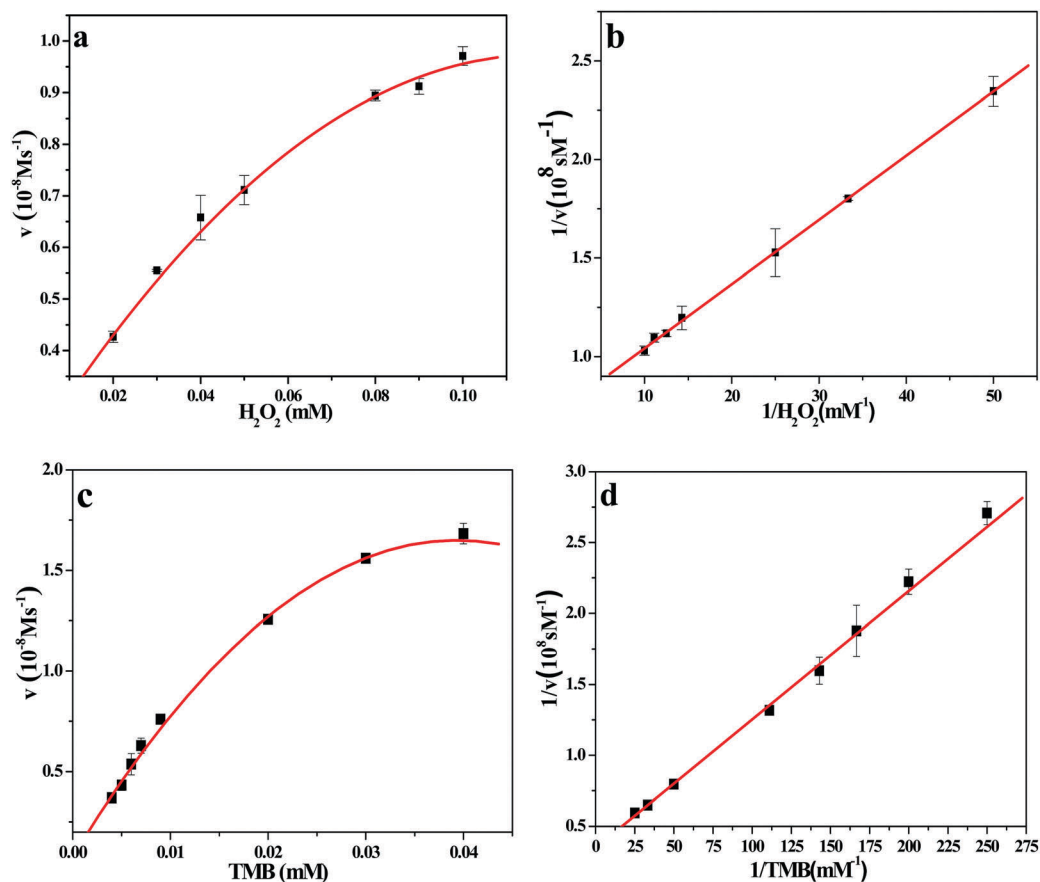


Fig. 7 Steady-state kinetics assay of Por-ZnFe₂O₄ HSSs. (a) The concentration of TMB was 0.3 mM while the H₂O₂ was varied; (c) the concentration of H₂O₂ was 0.1 M while the TMB was varied; (b) and (d) double reciprocal plots of the activity of Por-ZnFe₂O₄ HSSs at a fixed concentration of one substrate versus varying concentration of the second substrate for H₂O₂ and TMB, respectively.

concentration of Por-ZnFe₂O₄ HSS. Following the adsorption of H₂O₂ onto the surface of Por-ZnFe₂O₄ HSS in the catalytic system, the O–O bond was broken into highly reactive •OH, catalyzed by the nanomaterials. The generated •OH oxidized TMB into the typical blue color. As a result, it was verified that the peroxidase-like activity of Por-ZnFe₂O₄ HSS actually originates from •OH radical generation, as shown in Scheme 2.

Our results indicate that the peroxidase-like activity of the Por-ZnFe₂O₄ nanocomposites is higher than that of ZnFe₂O₄ HSS. The reason is attributed to the synergistic effect of porphyrin molecules and the ZnFe₂O₄ HSS, similar to our previous study on porphyrin functionalized Fe₃O₄.^{45b} Scheme 2 shows the synergistic effect in the enhanced peroxidase-like activity of the Por-ZnFe₂O₄ HSS. Firstly, the photo-induced electrons can be easily transferred from the LUMO of the porphyrin to the conduction band (CB) of ZnFe₂O₄ owing to the lower CB level of ZnFe₂O₄. Since the high conductivity of ZnFe₂O₄ suppresses the direct recombination of photo-induced electron–hole pairs in Por-ZnFe₂O₄ HSS, the concentration of the active electrons in the CB of ZnFe₂O₄ increased continuously. Therefore, the active electrons could efficiently reduce the H₂O₂ adsorbed on Por-ZnFe₂O₄ HSS into hydroxyl radicals to achieve enhanced peroxidase-like activity.

3.4. Optimization of experimental conditions

Like other nanomaterial-based peroxidase mimetics and HRP, the catalytic activity of Por-ZnFe₂O₄ HSS was also dependent on the pH and temperature. Consequently, the effect of pH value

and temperature on the catalytic activity of Por-ZnFe₂O₄ HSS was investigated. By varying the pH from 2.0 to 9.0 and the temperature from 20 °C to 60 °C, the experiments were carried out by incubating a solution containing 40 μg mL⁻¹ Por-ZnFe₂O₄ HSS, 300 μM TMB and 0.01 M H₂O₂ for 3 min. Por-ZnFe₂O₄ HSS show pH and temperature-dependent catalytic activity (Fig. 6), and the optimal pH and temperature for peroxidase mimetics were 4.0 and 35 °C, respectively. From Fig. S3 (ESI†), it was found that the absorption intensity increased with increasing TMB concentration, but no obvious increase was observed when the concentration was higher than 0.3 mM. In the subsequent experiments, 0.3 mM was suggested as an optimized TMB concentration.

3.5. Kinetics analysis

Under the optimal conditions, the kinetics mechanism of Por-ZnFe₂O₄ HSS was studied by changing the concentrations of TMB and H₂O₂ respectively. The apparent steady-state kinetics data for this catalytic reaction were collected by varying the concentration of one substrate while keeping the other constant. Fig. 7 shows typical Michaelis–Menten curves recorded by varying the concentration of TMB or H₂O₂. It was observed that the oxidation reaction catalyzed by the Por-ZnFe₂O₄ HSS follows typical Michaelis–Menten behavior towards both TMB and H₂O₂ (Fig. 7a and c). The Lineweaver–Burk double reciprocal plots (Fig. 7b and d) show a good linear relationship between 1/v and 1/[S].

K_m is commonly identified as an indicator of enzyme affinity for substrates and a smaller value of K_m means a stronger affinity between the enzyme and the substrate and *vice versa*. The K_m values of Por-ZnFe₂O₄ HSS with H₂O₂ and TMB as substrates were calculated to be 0.045 mM and 0.026 mM, respectively. For comparison, Table 2 lists the K_m and V_{max} values of Por-ZnFe₂O₄ HSS, HRP and other nanomaterials. Clearly, it can be seen that the K_m values of Por-ZnFe₂O₄ HSS with both H₂O₂ and TMB as substrates were much smaller than those for reported HRP,² Fe₃O₄ MNPs,² ZnFe₂O₄ MNPs³⁶ and MoS₂-Pt₇₄Ag₂₆,⁵¹ suggesting that Por-ZnFe₂O₄ HSS exhibited

Table 2 Comparison of the apparent Michaelis constant (K_m) and maximum reaction rate (V_{max})

Catalyst	K_m [mM]		V_{max} [10^{-8} ms ⁻¹]		Ref.
	H ₂ O ₂	TMB	H ₂ O ₂	TMB	
HRP	3.7	0.434	8.71	10.00	2
Fe ₃ O ₄ MNPs	154	0.098	9.78	3.44	2
ZnFe ₂ O ₄ MNPs	1.66	0.85	7.74	13.31	36
MoS ₂ -Pt ₇₄ Ag ₂₆	0.386	25.71	3.22	7.29	51
Por-ZnFe ₂ O ₄ HSS	0.045	0.026	1.4	2.88	This work

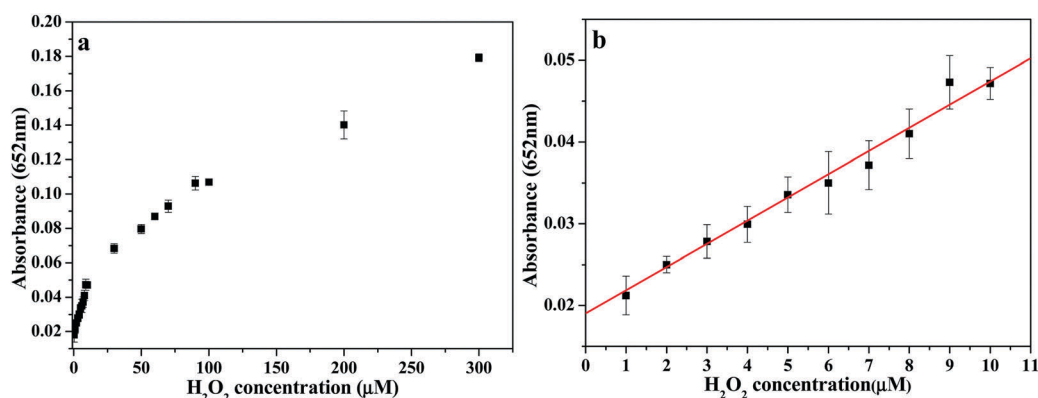
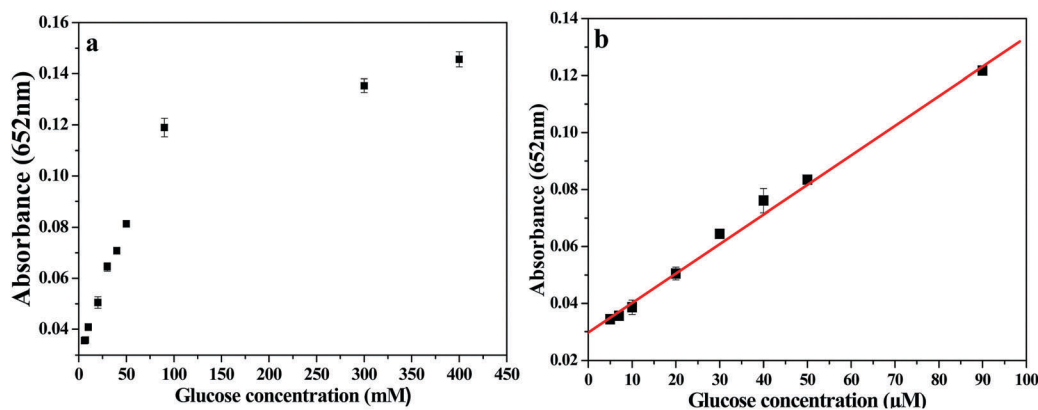


Fig. 8 (a) A dose–response curve for H₂O₂ detection using Por-ZnFe₂O₄ HSS as catalysts. (b) A linear calibration plot for H₂O₂ detection. Error bars represent the standard deviation based on three repeated measurements.

Table 3 Comparison of the linear range and LOD of this work with other materials as peroxidase mimics for the colorimetric detection of H₂O₂ and glucose

Peroxidase mimics	Linear range (μM) for		LOD (μM) for		Ref.
	H ₂ O ₂ detection	Glucose detection	H ₂ O ₂ detection	Glucose detection	
Fe ₃ O ₄ MNPs	5–100	50–1000	3	30	8
Cu ₂ (OH) ₃ Cl–CeO ₂	20–50	100–2000	10	50	52
MnSe-g-C ₃ N ₄ nanosheets	18–1800	0.16–1600	1.8	8	53
Cu NCs	10–1000	100–2000	10	100	4
Dichlorofluorescein	5–600	80–1200	2	30	21
Por–ZnFe ₂ O ₄ HSs	1–10	6–90	0.86	5.5	This work

**Fig. 9** (a) A dose–response curve for glucose detection using Por–ZnFe₂O₄ HSs as peroxidase mimics and (b) the linear calibration plot for glucose. The error bars represent the standard deviation of three measurements.

higher affinity toward both substrates than natural peroxidase HRP and the nanomaterials as peroxidase mimics listed in Table 2.

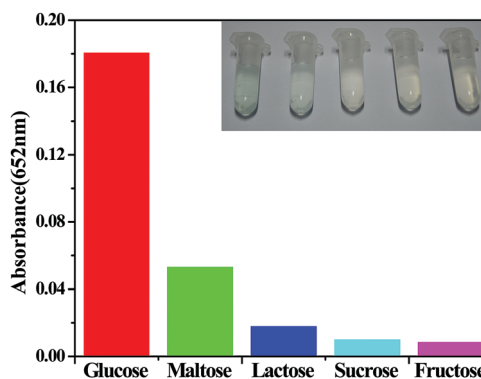
3.6. Detection of H₂O₂ and glucose

Based on the intrinsic peroxidase-like activity of Por–ZnFe₂O₄ HSs, we designed a simple colorimetric method for the determination of H₂O₂ and glucose. Since the absorbance at 652 nm of oxidized TMB is H₂O₂ concentration-dependent, it is straightforward to detect H₂O₂ using a UV-vis spectrophotometer or only the naked eye. Fig. 8a shows a H₂O₂ concentration–response curve in the range from 1 to 300 μM . A linear relationship between the absorbance and H₂O₂ concentration from 1 to 10 μM ($R^2 = 0.996$) was obtained with a detection limit of 0.86 μM (Fig. 8b). Furthermore, compared to other nanomaterials with peroxidase-like activity shown in Table 3, this method exhibits a reasonable linear range and a lower detection limit for H₂O₂.

Since H₂O₂ is the main product of the GOx-catalyzed reaction of glucose oxidation, the colorimetric detection of glucose can be realized when replacing HRP with the Por–ZnFe₂O₄ HSs. Considering the instability of GOx in pH 4.0 buffer solution, glucose detection can be performed as follows: (1) glucose is catalyzed by GOx to produce H₂O₂ and glucose acid in a pH 7.0 buffer solution; (2) Por–ZnFe₂O₄ HSs catalyze the oxidation of TMB in the presence of H₂O₂ at pH 4.0 to produce a blue colored mixture. Fig. 9 shows the standard response curve and the corresponding calibration plot for glucose. Compared with other materials shown in Table 3, this assay shows a linear range from

6 to 90 μM ($R^2 = 0.998$) with a detection limit as low as 5.5 μM . The comparative results indicate great potential for the rapid and sensitive analysis of glucose. In addition, the small error bars of the data show the high working reliability and good repeatability of the colorimetric method.

To further test the specificity of the proposed colorimetric method for the detection of glucose, other saccharides, such as maltose, lactose, sucrose and fructose, were used to replace glucose. Fig. 10 shows that the absorbance at 652 nm of oxidized TMB with glucose is obviously higher than that of other glucose analogs,

**Fig. 10** Selectivity analysis for glucose detection by monitoring the absorbance at 652 nm with the colorimetric method using GOx and the as-prepared the Por–ZnFe₂O₄ HSs (from left to right: 1 mM glucose, 5 mM maltose, 5 mM lactose, 5 mM sucrose, and 5 mM fructose). Inset: The color change for the different samples.

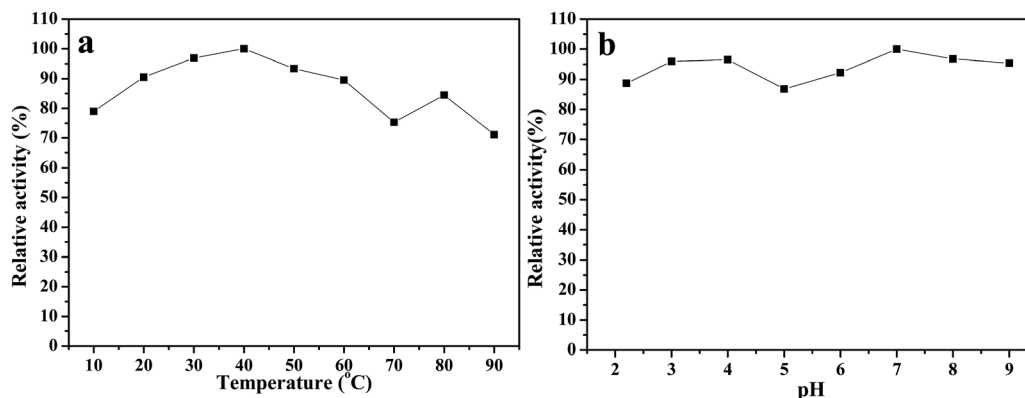


Fig. 11 Relative catalytic activity of the Por-ZnFe₂O₄ HSs after incubation at a range of temperatures (10–90 °C) (a) and a range of pH values (2.0–9.0) (b) for 2 h. The maximum point in each curve is set as 100%.

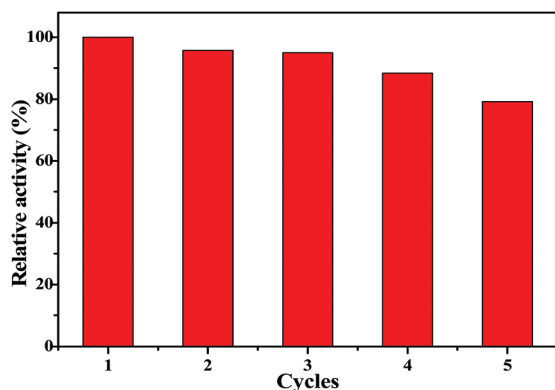


Fig. 12 Relative catalytic activity of the Por-ZnFe₂O₄ HSs in 5 successive catalysis cycles.

although the concentration of these analogs is about 5 times higher than that of glucose. This indicates that the proposed method is extremely selective for glucose. The detection of glucose can be realized conveniently through the color change that is observable by the naked eye, and the good selectivity of Por-ZnFe₂O₄ HSs towards glucose is confirmed.

3.7. Robustness of the peroxidase-like activity of Por-ZnFe₂O₄ HSs

For practical applications, the stability of peroxidase mimetics over broad pH and temperature ranges is of great importance. Therefore, we herein investigated the robustness of Por-ZnFe₂O₄ HS nanocomposites. Por-ZnFe₂O₄ HSs were incubated at different temperatures (10–90 °C) and pH values (2.0–9.0) for 2 h and their activities were then measured. Fig. 11a shows that the activity of Por-ZnFe₂O₄ HSs remains stable over a wide temperature range from 10 °C to 90 °C. When incubated in solutions with different pH values, the maximum activity of Por-ZnFe₂O₄ HSs exhibits no significant change (Fig. 11b). This is in contrast to HRP where, after being incubated at a pH lower than 5.0 or a temperature higher than 40 °C for 2 h, the catalytic activity decreased sharply.

To investigate the recyclability of Por-ZnFe₂O₄ HSs, experiments were performed by conducting the peroxidase mimetic experiments successively for 5 cycles. After each cycle, the Por-ZnFe₂O₄

HSs were collected using a magnet and after being washed with deionized water, the Por-ZnFe₂O₄ HSs samples were reused in the next cycle. From the data shown in Fig. 12, it can be concluded that only a slight decline in relative activity was observed after 5 cycles. In conclusion, the good stability and reusability of the Por-ZnFe₂O₄ HSs is suitable for wide use in the biochemistry and environmental protection fields.

4. Conclusion

In summary, we have reported the preparation of porphyrin functionalized magnetic ZnFe₂O₄ HSs through a facile one-pot hydrothermal process. They could rapidly catalyze the oxidation of TMB by H₂O₂ to produce a typical blue colored solution and the catalytic activity was strongly dependent on pH and temperature. As a peroxidase mimic, the nanocomposites show several advantages over natural enzymes and other nanozymes. Furthermore, owing to the synergistic effect of porphyrin molecules and ZnFe₂O₄ HSs, the •OH radicals played a major role in the peroxidase mimetic catalytic reaction, as indicated by the ESR results. The synthesized organic-inorganic nanocomposite based glucose colorimetric method is simple, cheap, convenient, highly selective, sensitive, and easy to handle. Based on our investigations, it is expected that great potential applications of the nanocomposites may be found in biotechnology, environmental chemistry and other related fields.

Conflicts of interest

There are no conflicts to declare.

Acknowledgements

Financial support provided for this research by the National Natural Science Foundation of China (Grant No. 21271119), the Natural Science Foundation of Shandong Province (Grant No. ZR2018MB002 and ZR2018MEE003) and the Taishan Scholars Projects of Shandong (No. ts201511033) is gratefully acknowledged.

References

- 1 Y. Lin, J. Ren and X. G. Qu, Catalytically active nanomaterials: a promising candidate for artificial enzymes, *Acc. Chem. Res.*, 2014, **47**, 1097–1105.
- 2 L. Z. Gao, J. Zhuang, L. Nie, J. B. Zhang, Y. Zhang, N. Gu, T. H. Wang, J. Feng, D. L. Yang, S. Perrett and X. Y. Yan, Intrinsic peroxidase-like activity of ferromagnetic nanoparticles, *Nat. Nanotechnol.*, 2007, **2**, 577–583.
- 3 Y. Jv, B. X. Li and R. Cao, Positively-charged gold nanoparticles as peroxidase mimic and their application in hydrogen peroxide and glucose detection, *Chem. Commun.*, 2010, **46**, 8017–8019.
- 4 L. Z. Hu, Y. L. Yuan, L. Zhang, J. M. Zhao, S. Majeed and G. B. Xu, Copper nanoclusters as peroxidase mimetics and their applications to H₂O₂ and glucose detection, *Anal. Chim. Acta*, 2013, **762**, 83–86.
- 5 M. L. Cui, J. D. Zhou, Y. Zhao and Q. J. Song, Facile synthesis of iridium nanoparticles with superior peroxidase-like activity for colorimetric determination of H₂O₂ and xanthine, *Sens. Actuators, B*, 2017, **243**, 203–210.
- 6 L. H. Jin, Z. Meng, Y. Q. Zhang, S. J. Cai, Z. H. Zhang, C. Li, L. Shang and Y. H. Shen, Ultrasmall Pt nanoclusters as robust peroxidase mimics for colorimetric detection of glucose in human serum, *ACS Appl. Mater. Interfaces*, 2017, **9**, 10027–10033.
- 7 J. S. Mu, Y. Wang, M. Zhao and L. Zhang, Intrinsic peroxidase-like activity and catalase-like activity of Co₃O₄ nanoparticles, *Chem. Commun.*, 2012, **48**, 2540–2542.
- 8 H. Wei and E. Wang, Fe₃O₄ magnetic nanoparticles as peroxidase mimetics and their applications in H₂O₂ and glucose detection, *Anal. Chem.*, 2008, **80**, 2250–2254.
- 9 F. Natalio, R. André, A. F. Hartog, B. Stoll, K. P. Jochum, R. Wever and W. Tremel, Vanadium pentoxide nanoparticles mimic vanadium haloperoxidases and thwart biofilm formation, *Nat. Nanotechnol.*, 2012, **7**, 530–535.
- 10 X. R. Guo, Y. Wang, F. Y. Wu, Y. N. Ni and S. Kokotc, A colorimetric method of analysis for trace amounts of hydrogen peroxide with the use of the nano-properties of molybdenum disulfide, *Analyst*, 2015, **140**, 1119–1126.
- 11 T. R. Lin, L. S. Zhong, H. Chen, Z. H. Li, Z. P. Song, L. Q. Guo and F. F. Fu, A sensitive colorimetric assay for cholesterol based on the peroxidase-like activity of MoS₂ nanosheets, *Microchim. Acta*, 2017, **184**, 1233–1237.
- 12 T. R. Lin, L. S. Zhong, Z. P. Song, L. Q. Guo, H. Y. Wu, Q. Q. Guo, Y. Chen, F. F. Fu and G. G. Chen, Visual detection of blood glucose based on peroxidase-like activity of WS₂ nanosheets, *Biosens. Bioelectron.*, 2014, **62**, 302–307.
- 13 Z. H. Dai, S. H. Liu, J. C. Bao and H. X. Ju, Nanostructured FeS as a mimic peroxidase for biocatalysis and biosensing, *Chem. – Eur. J.*, 2009, **15**, 4321–4326.
- 14 Y. J. Song, K. G. Qu, C. Zhao, J. S. Ren and X. G. Qu, Graphene oxide: intrinsic peroxidase catalytic activity and its application to glucose detection, *Adv. Mater.*, 2010, **22**, 2206–2210.
- 15 W. B. Shi, Q. L. Wang, Y. J. Long, Z. L. Cheng, S. H. Chen, H. Z. Zheng and Y. M. Huang, Carbon nanodots as peroxidase mimetics and their applications to glucose detection, *Chem. Commun.*, 2011, **47**, 6695–6697.
- 16 Y. J. Long, X. L. Wang, D. J. Shen and H. Z. Zheng, Detection of glucose based on the peroxidase-like activity of reduced state carbon dots, *Talanta*, 2016, **159**, 122–126.
- 17 S. Y. Zhu, X. E. Zhao, J. M. You, G. B. Xu and H. Wang, Carboxylic-group-functionalized single-walled carbon nanohorns as peroxidase mimetics and their application to glucose detection, *Analyst*, 2015, **140**, 6398–6403.
- 18 R. M. Li, M. M. Zhen, M. R. Guan, D. Q. Chen, G. Q. Zhang, J. C. Ge, P. Gong, C. R. Wang and C. Y. Shu, A novel glucose colorimetric sensor based on intrinsic peroxidase-like activity of C₆₀-carboxyfullerenes, *Biosens. Bioelectron.*, 2013, **47**, 502–507.
- 19 Y. Tao, E. G. Ju, J. S. Ren and X. G. Qu, Polypyrrole nanoparticles as promising enzyme mimics for sensitive hydrogen peroxide detection, *Chem. Commun.*, 2014, **50**, 3030–3032.
- 20 M. Liu, B. X. Li and X. Cui, Anionic polythiophene derivative as peroxidase mimetics and their application for detection of hydrogen peroxide and glucose, *Talanta*, 2013, **115**, 837–841.
- 21 M. L. Li, L. Liu, Y. Shi, Y. F. Yang, H. Z. Zheng and Y. J. Long, Dichlorofluorescein as a peroxidase mimic and its application to glucose detection, *New J. Chem.*, 2017, **41**, 7578–7582.
- 22 J. He, F. J. Xu, J. Hu, S. L. Wang, X. D. Hou and Z. Long, Covalent triazine framework-1: A novel oxidase and peroxidase mimic, *Microchem. J.*, 2017, **135**, 91–99.
- 23 X. Q. Lin, H. H. Deng, G. W. Wu, H. P. Peng, A. L. Liu, X. H. Lin, X. H. Xia. and W. Chen, Platinum nanoparticles/graphene-oxide hybrid with excellent peroxidase-like activity and its application for cysteine detection, *Analyst*, 2015, **140**, 5251–5256.
- 24 G. Darabdhara, B. Sharma, M. R. Das, R. Boukherroub and S. Szunerits, Cu-Ag bimetallic nanoparticles on reduced graphene oxide nanosheets as peroxidase mimic for glucose and ascorbic acid detection, *Sens. Actuators, B*, 2017, **238**, 842–851.
- 25 Y. F. Zhang, C. L. Xu and B. X. Li, Self-assembly of hemin on carbon nanotube as highly active peroxidase mimetic and its application for biosensing, *RSC Adv.*, 2013, **3**, 6044–6050.
- 26 Y. Tao, E. G. Ju, J. S. Ren and X. G. Qu, Bifunctionalized mesoporous silica-supported gold nanoparticles: intrinsic oxidase and peroxidase catalytic activities for antibacterial applications, *Adv. Mater.*, 2015, **27**, 1097–1104.
- 27 N. S. Surgutskaya, M. E. Trusova, G. B. Slepchenko, A. S. Minin, A. G. Pershina, M. A. Uimin, A. E. Yermakov and P. S. Postnikov, Iron-core/carbon-shell nanoparticles with intrinsic peroxidase activity: new platform for mimetic glucose detection, *Anal. Methods*, 2017, **9**, 2433–2439.
- 28 D. Jampaiah, T. S. Reddy, V. E. Coyle, A. Nafady and S. K. Bhargava, Co₃O₄@CeO₂ hybrid flower-like microspheres: a strong synergistic peroxidase-mimicking artificial enzyme with high sensitivity for glucose detection, *J. Mater. Chem. B*, 2017, **5**, 720–730.
- 29 (a) Y. J. Chen, H. Y. Cao, W. B. Shi, H. Liu and Y. M. Huang, Fe-Co bimetallic alloy nanoparticles as a highly active

- peroxidase mimetic and its application in biosensing, *Chem. Commun.*, 2013, **49**, 5013–5015; (b) Y. Lu, W. C. Ye, Q. Yang, J. Yu, Q. Wang, P. P. Zhou, C. M. Wang, D. S. Xue and S. Q. Zhao, Three-dimensional hierarchical porous PtCu dendrites: A highly efficient peroxidase nanozyme for colorimetric detection of H₂O₂, *Sens. Actuators, B*, 2016, **230**, 721–730.
- 30 Y. N. Ding, B. C. Yang, H. Liu, Z. Liu, X. Zhang, X. W. Zheng and Q. Y. Liu, FePt-Au ternary metallic nanoparticles with the enhanced peroxidase-like activity for ultrafast colorimetric detection of H₂O₂, *Sens. Actuators, B*, 2018, **259**, 775–783.
- 31 S. J. Liu, J. W. Fu, M. H. Wang, Y. Yan, Q. Q. Xin, L. Cai and Q. Xu, Magnetically separable and recyclable Fe₃O₄-polydopamine hybrid hollow microsphere for highly efficient peroxidase mimetic catalysts, *J. Colloid Interface Sci.*, 2016, **469**, 69–77.
- 32 M. M. Chen, L. F. Sun, Y. N. Ding, Z. Q. Shi and Q. Y. Liu, N,N'-Di-carboxymethyl perylene diimide functionalized magnetic nanocomposites with enhanced peroxidase-like activity for colorimetric sensing of H₂O₂ and glucose, *New J. Chem.*, 2017, **41**, 5853–5862.
- 33 H. Song, L. P. Zhu, Y. G. Li, Z. R. Lou, M. Xiao and Z. Z. Ye, Preparation of ZnFe₂O₄ nanostructures and highly efficient visible-light-driven hydrogen generation with the assistance of nanoheterostructures, *J. Mater. Chem. A*, 2015, **3**, 8353–8360.
- 34 A. Sutka, J. Zavickis, G. Mezinskas, D. Jakovlevs and J. Barloti, Ethanol monitoring by ZnFe₂O₄ thin film obtained by spray pyrolysis, *Sens. Actuators, B*, 2013, **176**, 330–334.
- 35 J. Q. Wan, X. H. Jiang, H. Li and K. Z. Chen, Facile synthesis of zinc ferrite nanoparticles as non-lanthanide T₁ MRI contrast agents, *J. Mater. Chem.*, 2012, **22**, 13500–13505.
- 36 L. Su, J. Feng, X. M. Zhou, C. L. Ren, H. H. Li and X. G. Chen, Colorimetric detection of urine glucose based ZnFe₂O₄ magnetic nanoparticles, *Anal. Chem.*, 2012, **2012**, 5753–5758.
- 37 R. A. W. Johnstone, A. J. Simpson and P. A. Stocks, Heterobimetallic cycloheptatrienyl and cycloheptatrienyldene complexes, *Chem. Commun.*, 1997, 2277–2278.
- 38 X. H. Wang, K. G. Qu, B. L. Xu, J. S. Ren and X. G. Qu, Multicolor luminescent carbon nanoparticles: synthesis, supramolecular assembly with porphyrin, intrinsic peroxidase-like catalytic activity and applications, *Nano Res.*, 2011, **4**, 908–920.
- 39 R. X. Wang, J. J. Fan, Y. J. Fan, J. P. Zhong, L. Wang, S. G. Sun and X. C. Shen, Platinum nanoparticles on porphyrin functionalized graphene nanosheets as a superior catalyst for methanol electrooxidation, *Nanoscale*, 2014, **6**, 14999–15007.
- 40 C. M. Drain, A. Varotto and I. Radivojevic, Self-organized porphyrinic materials, *Chem. Rev.*, 2009, **109**, 1630–1658.
- 41 Y. Z. Chen, C. Y. Zhang, X. J. Zhang, X. M. Ou and X. H. Zhang, One-step growth of organic single-crystal p-n nano-heterojunctions with enhanced visible-light photocatalytic activity, *Chem. Commun.*, 2013, **59**, 9200–9202.
- 42 (a) R. A. W. Johnstone, A. J. Simpson and P. A. Stocks, Porphyrins in aqueous amphiphilic polymers as peroxidase mimics, *Chem. Commun.*, 1997, 2277–2278; (b) Y. F. Huan, Q. Fei, H. Y. Shan, B. J. Wang, H. Xu and G. D. Feng, A novel water-soluble sulfonated porphyrin fluorescence sensor for sensitive assays of H₂O₂ and glucose, *Analyst*, 2015, **140**, 1655–1661.
- 43 (a) M. J. Lv, T. Mei, C. A. Zhang and X. B. Wang, Selective and sensitive electrochemical detection of dopamine based on water-soluble porphyrin functionalized graphene nanocomposites, *RSC Adv.*, 2014, **4**, 9261–9270; (b) M. S. Zhu, Z. Li, B. Xiao, Y. T. Lu, Y. K. Du, P. Yang and X. M. Wang, Surfactant assistance in improvement of photocatalytic hydrogen production with the porphyrin noncovalently functionalized graphene nanocomposite, *ACS Appl. Mater. Interfaces*, 2013, **5**, 1732–1740.
- 44 W. W. Tu, J. P. Lei, P. Wang and H. X. Ju, Photoelectrochemistry of free-base-porphyrin-functionalized zinc oxide nanoparticles and their applications in biosensing, *Chem. – Eur. J.*, 2011, **17**, 9440–9447.
- 45 (a) Q. Y. Liu, Y. T. Yang, H. Li, R. R. Zhu, Q. Shao, S. G. Yang and J. J. Xu, NiO nanoparticles modified with 5, 10, 15, 20-tetrakis(4-carboxylphenyl)-porphyrin: promising peroxidase mimetics for H₂O₂ and glucose detection, *Biosens. Bioelectron.*, 2015, **64**, 147–153; (b) Q. Y. Liu, H. Li, Q. R. Zhao, R. R. Zhu, Y. Y. Yang, Q. Y. Jia, B. Bian and L. H. Zhuo, Glucose-sensitive colorimetric sensor based on peroxidase mimics activity of porphyrin-Fe₃O₄ nanocomposites, *Mater. Sci. Eng., C*, 2014, **41**, 142–151; (c) Q. Y. Liu, Y. T. Yang, X. T. Lv, Y. Y. Ding, Y. Zhang, J. J. Jing and C. Xu, One-step synthesis of uniform nanoparticles of porphyrin functionalized ceria with promising peroxidase mimetics for H₂O₂ and glucose colorimetric detection, *Sens. Actuators, B*, 2017, **240**, 726–734.
- 46 (a) Q. Y. Liu, P. P. Chen, Z. Xu, M. M. Chen, Y. N. Ding, K. Yue and J. Xu, A facile strategy to prepare porphyrin functionalized ZnS nanoparticles and their peroxidase-like catalytic activity for colorimetric sensor of hydrogen peroxide and glucose, *Sens. Actuators, B*, 2017, **251**, 339–348; (b) Q. Y. Liu, Q. Y. Jia, R. R. Zhu, Q. Shao, D. M. Wang, P. Cui and J. C. Ge, 5,10,15,20-Tetrakis(4-carboxyl phenyl)-porphyrin-CdS nanocomposites with intrinsic peroxidase-like activity for glucose colorimetric detection, *Mater. Sci. Eng., C*, 2014, **42**, 177–184.
- 47 A. D. Adler, F. R. Longo, J. D. Finarelli, J. Goldmacher, J. Assour and L. Korsakoff, A simplified synthesis for meso-tetraphenylporphyrin, *J. Org. Chem.*, 1967, **32**, 476.
- 48 Y. L. Guo, X. Y. Liu, X. D. Wang, A. Lqbal, C. D. Yang, W. S. Liu and W. W. Qin, Carbon dot/NiAl-layered double hydroxide hybrid material: facile synthesis, intrinsic peroxidase-like catalytic activity and its application, *RSC Adv.*, 2015, **5**, 95495–95503.
- 49 Y. L. Dong, H. G. Zhang, Z. U. Rahman, L. Su, X. J. Chen, J. Hua and X. G. Chen, Graphene oxide-Fe₃O₄ magnetic nanocomposites with peroxidase-like activity for colorimetric detection of glucose, *Nanoscale*, 2012, **4**, 3969–3976.
- 50 (a) Z. W. Chen, J. J. Yin, Y. T. Zhou, Y. Zhang, L. Song, M. J. Song, S. L. Hu and N. Gu, Dual enzyme-like activities of

- iron oxide nanoparticles and their implication for diminishing cytotoxicity, *ACS Nano*, 2012, **6**, 4001–4012; (b) W. B. Shi, X. D. Zhang, S. H. He and Y. M. Huang, CoFe₂O₄ magnetic nanoparticles as a peroxidase mimic mediated chemiluminescence for hydrogen peroxide and glucose, *Chem. Commun.*, 2011, **47**, 10785–10787; (c) J. J. Guo, Y. Wang and M. Zhao, 3D flower-like ferrous(II) phosphate nanostructures as peroxidase mimetics for sensitive colorimetric detection of hydrogen peroxide and glucose at nanomolar level, *Talanta*, 2018, **182**, 230–240.
- 51 S. F. Cai, Q. S. Han, C. Qi, Z. Lian, X. H. Jia, R. Yang and C. Wang, Pt₇₄Ag₂₆ nanoparticles-decorated ultrathin MoS₂ nanosheets as novel peroxidase mimics for highly selective colorimetric detection of H₂O₂ and glucose, *Nanoscale*, 2016, **8**, 3685–3693.
- 52 N. Wang, J. C. Sun, L. J. Chen, H. Fan and S. Y. Ai, A Cu₂(OH)₃Cl-CeO₂ nanocomposite with peroxidase-like activity, and its application to the determination of hydrogen peroxide, glucose and cholesterol, *Microchim. Acta*, 2015, **182**, 1733–1738.
- 53 F. M. Qiao, Q. Q. Qi, Z. Z. Wang, K. Xu and S. Y. Ai, MnSe-loaded g-C₃N₄ nanocomposite with synergistic peroxidase-like catalysis: Synthesis and application toward colorimetric biosensing of H₂O₂ and glucose, *Sens. Actuators, B*, 2016, **229**, 379–386.